PROCEEDINGS OF THE INTERNATIONAL CONFERENCE
NANOMATERIALS: APPLICATIONS AND PROPERTIES
Vol. **3** No 1, 01PCSI08(5pp) (2014)

Femtosecond Laser Micro/nano Machining on Metallic and Semiconductor Materials

R. Kuladeep, L. Jyothi, and D. Narayana Rao*

School of Physics, University of Hyderabad, Hyderabad 500046, Andhra Pradesh, India

(Received 30 June 2014; published online 29 August 2014)

Formation of ripples or laser induced periodic surface structures (LIPSS) on semiconductor material like Silicon (Si) and on metals like Aluminum (Al) and Copper (Cu) and fabrication Silver (Ag) nanostructures in polymer matrix by femtosecond (fs) laser direct writing are reported in this paper. Laser irradiation was performed at normal incidence in air using linearly polarized Ti:Sapphire fs laser pulses of ~ 110 fs pulse duration and ~ 800 nm wavelength. Field emission scanning electron microscopy (FESEM) is utilized for imaging surface morphologies of laser written structures, revealing that surface morphology depends on various material processing parameters like laser fluence, polarization, material properties and number of applied pulses. Formation of polymer capped Ag nanoparticles inside the laser written microstructures is confirmed by the appearance of surface plasmon absorption band at 448 nm in the UV-Vis extinction spectrum. Nanoparticles formed were spherical in shape with an average particle size less than 20 nm. This technique is efficient, universal, cost-effective, and environmental friendly, which has potential applications in the fabrication of micro/nanostructures on variety of materials for microelectromechanical systems, nanoelectronics and nanophotonics.

Keywords: Modifications of solid, Laser, Micro/nanostructures, Nanoparticles, Surface.

PACS numbers: 78.67. – n, 81.16.Mk

1. INTRODUCTION

Laser-induced modifications of solid materials, particularly those limited on the sub-surface region, is used for material processing in many ways: forming stable nanoparticles [1], micro- and nano-scale machining in microelectronics [2], creating desired surface micro- and nano- patterns [3-4], and modifying the composition and chemical state of the irradiated surface [5]. Among the entire laser surface structuring techniques, direct feature writing using femtosecond (fs) laser has been touted as an excellent fabrication technique owing to its ease of operation and more importantly owing to the outcome which in turn facilitates the possibility of advance applications [6-7]. This technique also allows overcoming the limitations imposed by the diffraction limit in the definition of structures with periods below the incident laser wavelength. Laser-induced periodic surface structures (LIPSS) can be categorized into low spatial frequency LIPSS (LPSL) with orientation perpendicular to the laser beam polarization and periods close to the incident wavelength, and high spatial frequency LIPSS (HSFL), that appear with orientations both parallel and perpendicular to beam polarization, and periods that show values much smaller than those of LSFL, even reaching tens of nanometers.

Noble metal nanoparticles exhibit a wide variety of spectroscopic, electronic and chemical properties that find applications in various fields including electronics, photonics, plasmonics and sensing. Especially, polymer films embedded with metal nanoparticles offer unique optical and electrical properties. The polymer matrix serves not only as a medium to assemble the nanoparticles but also stabilize them against aggregation. These films make metal ions disperse uniformly preventing harmful diffusion of metal ions and surface of the resultant structure is likely to be smoother. In addition, film samples can be easily prepared and are feasible for electrical and optical applications. These properties are mainly determined by size, shape and spatial arrangement of the nanoparticles [8]. Methods which allow a modification of the nanostructure and the properties of these films in a controlled way are of great interest because they will enlarge the range of potential applications in optical and electronic industries.

Here in this letter we report the fabrication of LSFL on the surface of semiconductor material like Silicon (Si) and metals like Aluminium (Al) and Copper (Cu) by laser direct writing technique using near infrared fs laser pulses. We also report the formation of Silver (Ag) nanostructures fabricated in polymer matrix containing metal ions that, upon femtosecond laser irradiation, lead to the growth of nanoparticles into defined continuous metal particle structures.

2. EXPERIMENTAL DETAILS

A target of 1 mm thickness Al and Cu having purity of 99.99% was purchased from Aldrich and washed with ethanol and deionized water to remove organic dopants from the surface in an ultrasonic cleaner prior to the laser irradiation. Commercially available p-type (10–20 Ω cm) (1 1 1) Si wafers have been used in the experiments. The Si wafers were etched with 8% HF for 5 min to remove the native oxide layer on the surface. The laser source utilized in direct writing experiments was a Ti:Sapphire oscillator-amplifier system (Spectra Physics, Spitfire) operating at a wavelength of ~ 800 nm and delivering ~ 1 mJ output energy pulses at a repetition rate of 1 kHz. Duration of each laser pulse is about ~ 110 fs. The fs laser pulses are linearly

* dnrsp@uohyd.ernet.in, dnr_laserlab@yahoo.com

polarized. Neutral density filters and the combination of half wave plate and a polarizer were utilized to adjust the irradiation fluence. The laser beam was made to incident normal to the surface and focused by a microscopic objective lens with a numerical aperture of 0.25. Writing was performed transverse to the laser propagation direction. In order to account for the reflection losses of the lens all the energy/fluence measurements were performed after the lens. Computer controlled translational stages (Newport, USA) were arranged to translate the sample in x, y, and z directions. Scanning of the sample was done in both along and normal to the laser polarization direction. Samples were rinsed for 5 min in acetone after irradiation, in an ultrasonic cleaner in order to remove any debris formed during the ablation process. Detailed characterization of the morphological changes of the material surface after laser irradiation was performed by Zeiss ultra55 ultra high resolution field emission scanning electron microscope (FESEM) operated at an accelerating voltage of 5 kV.

3. RESULTS AND DISCUSSION

3.1 Formation of LIPSS on Si, Al and Cu

Fig. 1 shows FESEM images of surface morphological evolution on Si, Al and Cu irradiated with 800 nm linear polarized fs laser pulses with the irradiation fluence slightly higher than respective ablation thresholds. Direction of laser polarization and direction of sample translation are shown by solid arrow and dashed arrow, respectively. The characteristic properties of the LIPSS have been studied as function of laser parameters such as fluence, scanning speed (pulse number) and polarization. The results obtained have shown that the nanostructure is usually produced with multiple laser pulses at low fluence around the ablation threshold, where the periodic structures have their wave vectors parallel to the laser *E*-field. Surface morphology of Si with the function of fluence has been studied as shown in fig. 1(a) and 1(b). Inside the microstructure fabricated with fluence of 0.46 J/cm^2 and at 50 μm/sec writing speed, some aperiodic structures are formed at the center of the visible laser modified region, while long continuous LSFL are formed near the edges of the fabricated microstructure on the both sides as shown in fig.1(a). But at the same scanning speed with lower laser fluence of 0.3 J/cm^2 regular and continuous LSFL are observed all over the laser modified region. These results shows that the surface morphology of the laser irradiated surface depends on the laser fluence, a part of fluence, morphological features of the laser induced surface also depends on applied pulse number (scanning speed of the sample) and surrounding dielectric medium [3]. Surface morphology of Al after irradiation with fs laser pulses was shown in fig. 1(c) and 1(d). These results indicate the formation of LSFL and their orientations are perpendicular to the laser polarization, which is a remarkable characteristic for such an ultrafast laser induced nanostructures. Similar kind of LSFL formation was observed on Cu surface after fs laser irradiation as shown in fig. 1(e) and 1(f). In addition, our results with vertical and horizontal scanning of the sample demonstrate that the scanning direction has no influence on the orientation of the formed nanostructures.

Formation of sub-wavelength features on metal, dielectric and semiconductor has been well explained by the interference of laser with surface plasmon polaritons (SPPs) [9]. When irradiated with ultrashort laser pulses with damage threshold fluence, semiconductor or dielectric (or even metal) surface will form a thin layer in which incident laser pulse will predominantly produces a high density of free electrons N_e the optical properties of this excited material (thin layer) should be determined by abundant hot electrons rather than the intrinsic properties of solid material. This excited material layer including N_e works as a thin metal layer and supports the formation of SPPs which in turn undergo interference with the laser light leading to the formation of sub-wavelength features [10]. Spatial period (Λ) of the LIPSS formed by the interference of laser with SPPs under normal incidence of laser beam on the material surface is expressed as

$$\Lambda = \lambda_s = \lambda\left(\frac{\varepsilon' + \varepsilon_d}{\varepsilon'\varepsilon_d}\right)^{1/2},$$

where λ and λ_s are the wavelengths of incident laser and surface plasmons, ε' is the real part of the dielectric constant of the laser-excited material and ε_d is the dielectric constant of the surrounding dielectric material. In the present experiments the laser irradiation on the material surface was done in air and dielectric constant of air equals to 1(i.e., $\varepsilon_d = 1$). Therefore, the spatial period can be expressed as

$$\Lambda = \lambda_s = \lambda\left(1 + \frac{1}{\varepsilon'}\right)^{1/2}.$$

3.2 Fabrication of Ag nanostructures inside PVA matrix

Thin films of PVA (polyvinyl alcohol) + $AgNO_3$ were prepared by mixing the solutions of 50 mg of $AgNO_3$ dissolved in 10 ml of water and 225 mg of PVA (MW=88,000 g/mole) dissolved in 10 ml of water and stirring for 8h for complete miscibility in a dark room to avoid photodissociation of silver nitrate. Next, a 1ml aliquot solution was uniformly distributed on a 1x1cm^2 Si substrate or glass plate using the spin coating technique. These homogeneous films were dried in an oven for 2h at 30 ^{0}C. The thickness of the film was found to be ~ 2 μm. Fig. 2(a) shows the FESEM image of fs laser written microstructures on PVA+$AgNO_3$ thin film obtained by spin coating technique on Si substrate, with pulse energies ranging between 5 μJ to 1 μJ; below the energy threshold of 1 μJ we did not observe any microstructure formation. The patterns were created using horizontal polarized laser pulses, by translating the sample perpendicular to the laser propagation direction at 100 μm/sec scanning speed.

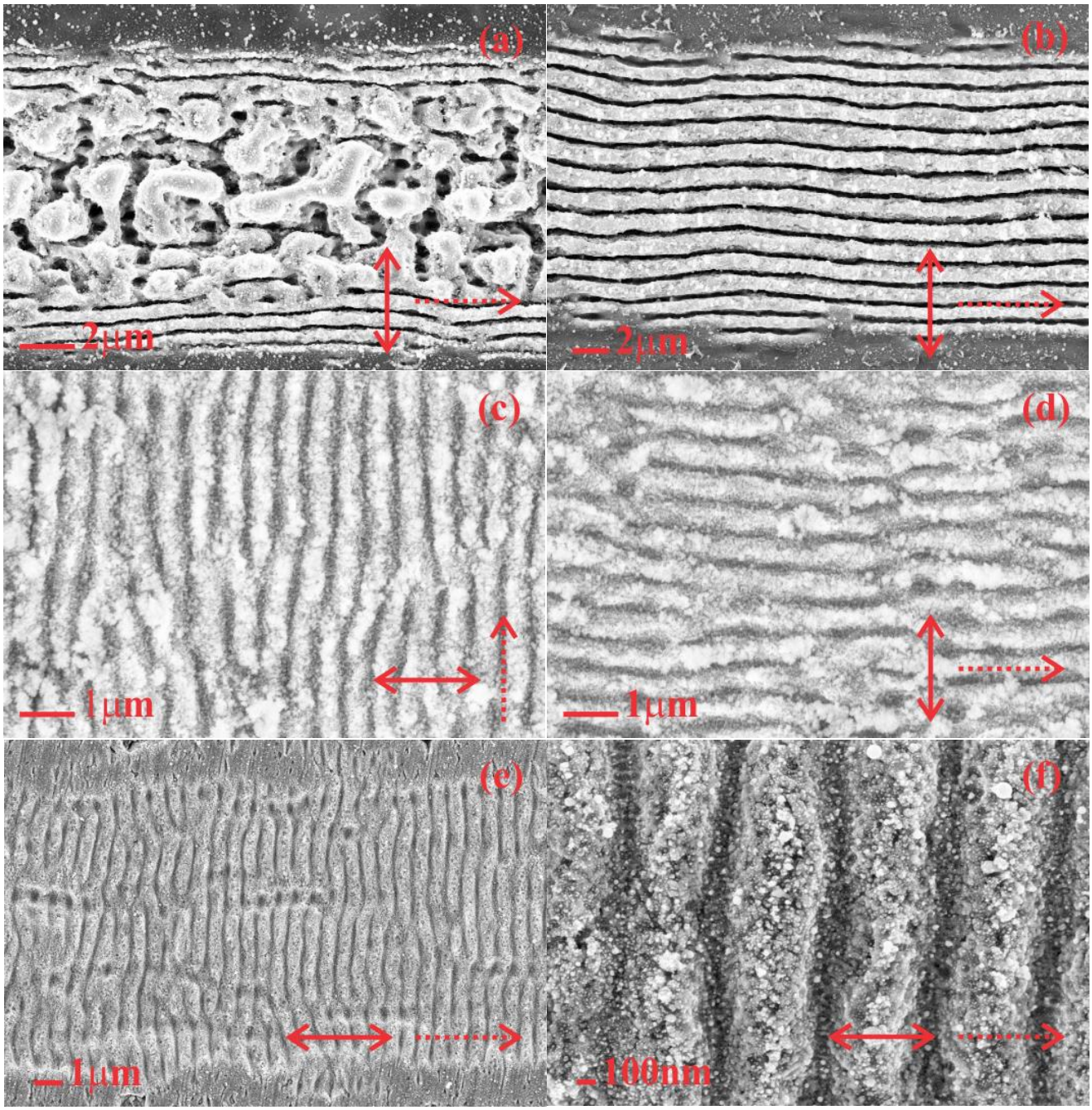

Fig. 1 – FESEM images of LIPSS produced by 800 nm fs laser linearly polarized pulses in air on (a), (b) Si, (c), (d) Al and (e), (f) Cu respectively. Laser polarization and writing directions are indicated by solid and dotted arrows, respectively.

Fig. 2 (b) shows the formation of spherical shaped Ag nanoparticles inside the microstructures that were fabricated with pulse energy of 5 μJ. Fig. 2(c) shows image of pristine (nonirradiated) region of $AgNO_3$+PVA thinfilm. The nanoparticles inside the fabricated microstructures are found to have polydispersity in size distribution, with an average particle size of 18 nm. Here, PVA acts simultaneously as the reducing agent [11-12] and as stabilizer for the Ag nanoparticles. PVA also plays the role of a matrix for homogeneous distribution and immobilization. In order to distinguish composition variation of irradiated area, we measured the UV-Vis absorption spectra. For UV-Vis absorption measurement, several structures were created close by, such as a grating in PVA+$AgNO_3$ thin film on glass substrate by focusing laser pulses with 10X objective. These structures were created by translating the sample at 100 μm/sec scanning speed and with pulse energy of 3 μJ. Unirradiated PVA+$AgNO_3$ thin film is transparent; the absorption spectra of these films show that there is no absorption peak in the visible region due to surface plasmon resonance of Ag nanoparticles. This confirms that the films do not contain any Ag nanoparticles before laser irradiation. Fig. 2(d) shows the extinction spectrum of fs laser inscribed grating film and the inset shows extinction spectrum of the freshly prepared film. After irradiation, formation of Ag nanoparticles was confirmed by the appearance of surface

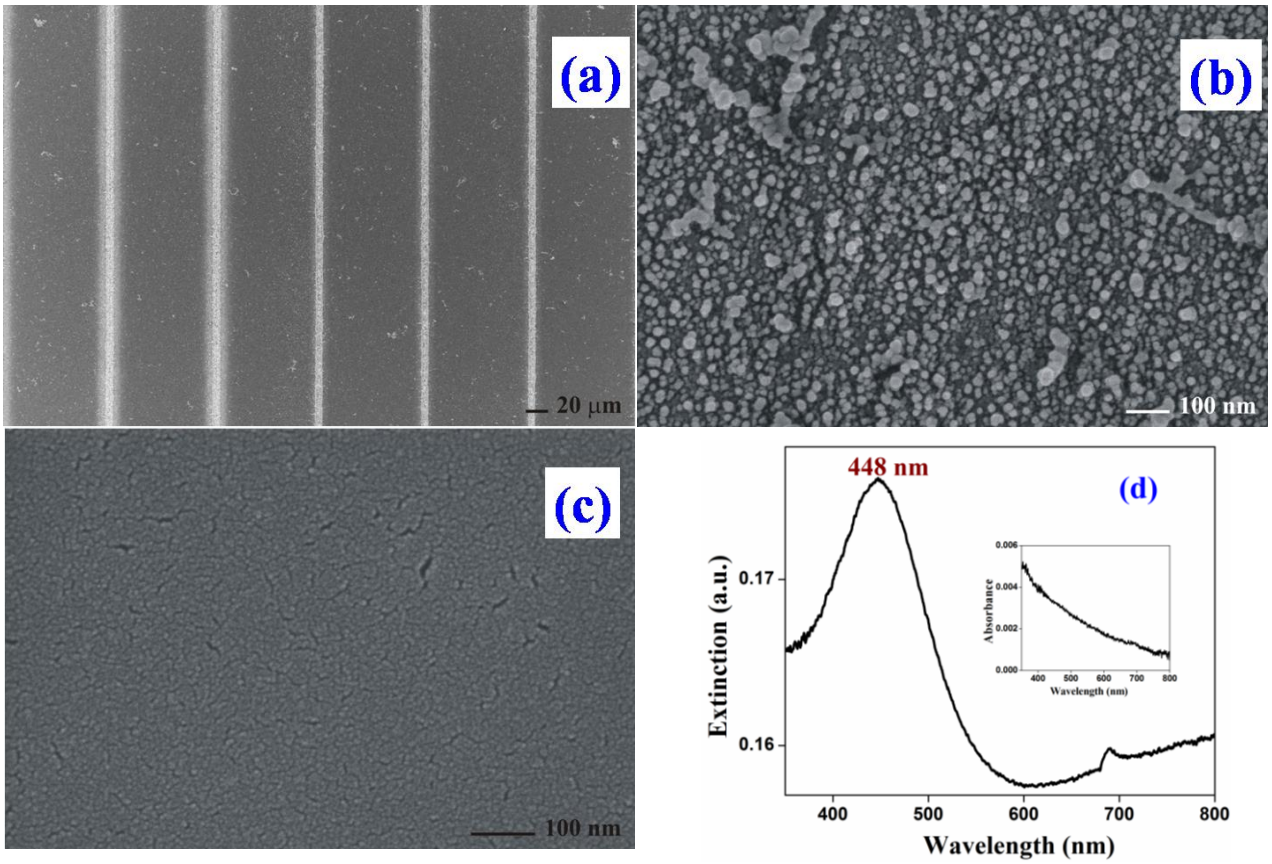

Fig. 2 – (a) FESEM images of representative photo deposited silver microstructures on $AgNO_3$ + PVA thin films with pulse energy ranging between 5 and 1 μJ. (b) Ag NPs inside the microstructures fabricated with 5 μJ. (c) FESEM image of pristine (nonirradiated) region of $AgNO_3$ + PVA thin film. (d) Extinction spectrum of femtosecond laser-inscribed grating on $AgNO_3$ + PVA film and inset shows extinction spectrum of the freshly prepared thin film.

plasmon peak centered at 448 nm in the UV-Vis absorption spectrum as shown in the fig. 2(d). It has been reported [12] that colloidal Ag nanoparticles have a similar absorption band, which is due to the surface plasmon absorption; the collective oscillation of free conduction electrons induced by the detecting light field in a metal particle [13]. The broad extinction spectrum confirms polydispersity in the constituent Ag nanoparticles size.

The key to our fabrication process is the chemical composition of the sample. In the process we present here, PVA was dissolved in water and cast as a thin film containing silver ions. By combining PVA and water, we obtain both a support matrix and controlled growth where PVA acts as both reducing and stabilizing agent. It is now well known that silver ions from the precursor, $AgNO_3$ get reduced by the hydroxyl groups of PVA when temperature of the mixture bath is raised [14]. The mechanism that takes place is as follows:

$$R_2CHOH \text{ (of the polymer)} + 2AgNO_3 \rightarrow R_2C{=}O + 2HNO_3 + 2Ag,$$

where R indicates the alkyl group of the polymer [15]. Our earlier studies [15] have shown that absorption of light complements the heating process as the absorbed photons raise the temperature of the sample irradiated through nonradiative processes. In the present studies, though there is no absorption at laser wavelength of 796 nm, we do see a strong absorption through two photon absorption (TPA) [16]. This TPA becomes stronger with the formation of the nanoparticles of Ag as Ag nanoparticles have absorption cross-section at around 450 nm. Due to diffusion process, the Ag ions aggregate forming Ag nanoparticles inside the fabricated microstructures.

4. CONCLUSIONS

In conclusion fs laser micro/nano machining on semiconductors, metals and metal doped polymer films is reported in this letter. Dependence of parameters like laser fluence, number of pulses irradiating the sample and laser polarization on the fs laser surface pattern is revealed in material processing. Formation of sub-wavelength structures is only possible within rather narrow range of laser fluences which are oriented perpendicular to laser polarization, while their surface morphology depends on processing parameters like laser fluence and number of applied pulses. We also present systematic investigation of fs laser induced formation of continuous Ag nano structures in thin polymer films containing Ag ions. The analysis of laser-irradiated films is mainly based on UV-Vis absorption spectrometer; electron microscopes clearly show that fabricated nanoparticles are spherical in shape with average particle size <20 nm exhibiting surface plasmon resonance at 448 nm.

REFERENCES

1. R. Kuladeep, L. Jyothi, P. Prakash, S. Mayank Shekhar, M. Durga Prasad and D. Narayana Rao, *J. Appl. Phys.* **114**, 243101 (2014).
2. E. Stratakis, R. Giorgi, M. Barberoglou, Th. Dikonimos, E. Salernitano, N. Lisi, and E. Kymakis, *Appl. Phys. Lett.* **96**, 043110 (2010).
3. R. Kuladeep, C. Sahoo, and D. Narayana Rao, *App. Phys.* **104**, 222103 (2014).
4. K. Mohan Kumar, R. Kuladeep, D. Narayana Rao, and V.V.S.S. Srikanth, *App. Phys. Lett.* **104**,161607 (2014).
5. K. Emmanuel, S. Kyriaki, M.S. Minas, F. Costas, and S. Emmanuel, *Adv. Funct. Mater.* **23**, 2742 (2013).
6. G. Della Valle, R. Osellame, and P. Laporta, J. *Opt. A: Pure Appl. Opt.* **11**, 013001 (2009).
7. S. Su, J. Li, G.C.B. Lee, S. Kate, D. Webb, and H. Ye, *Appl. Phys. Lett.* **102**, 231913 (2013).
8. U. Kreibig and M. Vollmer, *Optical Properties of Metal Clusters* (Springer-Verlag, Berlin: 1995).
9. M. Huang, F. Zhao, Y. Cheng, N. Xu, and Z. Xu, *Nano* **3** 12 (2009).
10. G. Miyaji, K. Miyazaki, K. Zhang, T. Yoshifuji, and J. Fujita, *Opt. Exp.* **20** 14848 (2012).
11. R. Kuladeep, L. Jyothi, K. Shadak Alee, K.L.N. Deepak, and D. Narayana Rao, *Opt. Mat. Exp.* **2** 161 (2012).
12. L. Longenberger, and G. Mills, *J. Phys. Chem.* **99**, 475 (1995).
13. S. Porel, S. Singh, and T. P. Radhakrishnan, *Chem. Commun.* **2005**, 2387 (2005).
14. G. C. Papavassiliou, Prog. *Solid State Chem.* **12**, 185 (1980).
15. K. Shadak Alee, R. Kuladeep, and, D. Narayana Rao, *Opt. Commun.* **293**, 69 (2013).
16. S. Porel, N. Venkatram, and D. Narayana Rao, T.P. Radhakrishnan, *J. Appl. Phys.* **102**, 033107 (2007).